BRNO UNIVERSITY OF TECHNOLOGY
VYSOKÉ UČENÍ TECHNICKÉ V BRNĚ

FACULTY OF ELECTRICAL ENGINEERING AND COMMUNICATION
FAKULTA ELEKTROTECHNIKY A KOMUNIKAČNÍCH TECHNOLOGIÍ

DEPARTMENT OF ELECTRICAL POWER ENGINEERING
ÚSTAV ELEKTROENERGETIKY

MONITORING AND SIMULATION OF ADS EXPERIMENTAL TARGET BEHAVIOUR, HEAT GENERATION, AND NEUTRON LEAKAGE

MONITORING A SIMULACE CHOVÁNÍ EXPERIMENTÁLNÍCH TERČŮ PRO ADS, VÝVINU TEPLA A ÚNIKU NEUTRONŮ

SHORTENED VERSION OF DOCTORAL THESIS
ZKRÁCENÁ VERZE DISERTAČNÍ PRÁCE

AUTHOR **Ing. JOSEF SVOBODA**
AUTOR PRÁCE

SUPERVISOR **doc. Ing. KAREL KATOVSKÝ, Ph.D.**
ŠKOLITEL

SUPERVISOR SPECIALIST **prom. fyz. JINDŘICH ADAM, CSc.**
ŠKOLITEL SPECIALISTA

Doctoral programme: Power Systems and Power Electronics

BRNO 2021

Keywords

accelerator-driven systems, ADS, ANSYS Fluent, data visualisation, experimental target heat generation, heat transfer, MCNPX, Python, spallation reaction, thermocouples

Klíčová slova

ADS, ANSYS Fluent, MCNPX, přenos tepla, Python, spalační reakce, vývin tepla experimentalních terčů, termočlánky, urychlovačem řízené systémy, vizualizace dat

Location of the PhD thesis storage:

Available at: Main Library of the FEEC, Branch II, Technická 12, 616 00 Brnoo

Místo uložení práce:

Práce je k dispozici: ve fakultní knihovně FEKT VUT v Brně, Technická 12, 602 00 Brno

ISBN:

Contents

Chapter 1

Introduction

Foreword - several subjective words, author's point of view.

Ecology. Economy. Energy.
Three important and well discussed topics, perceptibly connected, which politics across the globe deal with. In the last decade, the world and mostly European Union (EU) have finally begun to genuinely deal with ecology topics. During the developing of Europe, ecology was neglected and overlooked. Its economy was primarily built up on coal, crude oil, and natural gas. By growing the economy, we are still overlooking the nature needs. The planet Earth responds by rising sea levels, more frequent local droughts, increasing numbers of hurricanes, and other more frequent fluctuations. It is scientifically proved, the world is dealing with global warming, chiefly caused by human [1], [2].

We are growing in all ways. Economy, affluence, and so the population. We are losing track of sustainability and the sense of real wealth. We expect never-ending growth. We have great tools to communicate, to share knowledge and to get any seeking information. Maybe we were not ready for this information revolution. We are overwhelmed by information, we are enticed by populism. We are searching for a quick and easy solution. As the instant is not real, so the quick is not long lasting. The society polarisation is still growing, year by year, crisis by crisis. Independent newspapers are attacked worldwide.

Infinite affluence rising is not sustainable for all of 7.5 billion inhabitants of the planet Earth. Undeveloped countries are longing for a better future - economic growth - a piece of affluence they see on Facebook. There are many ideas and several certain ways to aim for the sustainable energy future. All of them start with the fossil fuels limitation, in particular coal. The energy sector is major, however, the incomplete combustion in household heating locally kills as well. Then the limitation of oil usage in transport and step-by-step reduction of the CO_2 emissions. We are facing many problems such as drought + clean water access + overpopulation $\rightarrow$ refugee crisis $\rightarrow$ disinformation + cyberattacks, and many others, including global warming and energy-ecology unsustainability.
▶ Developed countries must find an ecological solution for the growing undeveloped one.
In other ways, these economies will be grown by energy from fossil fuels which cause substantial problems for future generations. It is not about electricity production, it is a much deeper problem of primary energy usage.

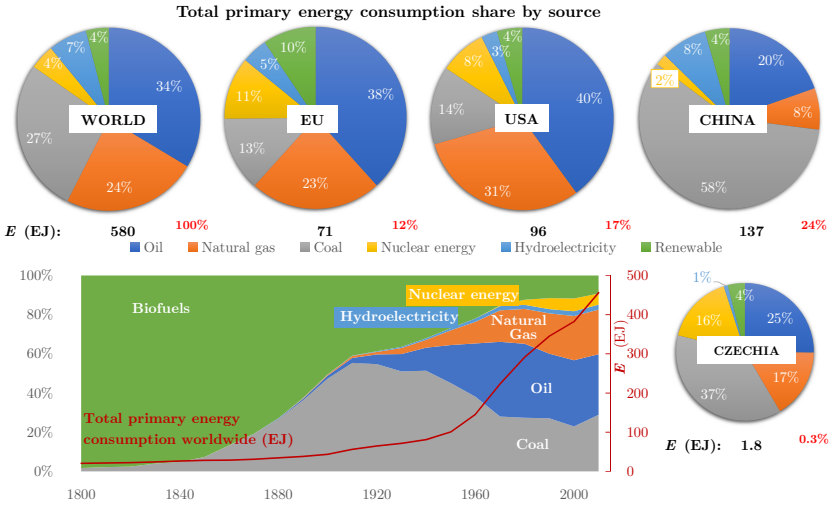

Figure 1.1: One of the most important charts to understand the primary energy consumption worldwide. Pie charts represent primary energy consumption by source per country, data 2018 [3]. Below pie charts is listed the annual energy consumption in [EJ] (black colour) and its relative ratio (red colour). The plane chart lower represents historical relative data of the primary energy share (left y axis by [%]). The total primary energy consumption word-wide is represented by red line the right y axis (red), data [4].

Generally, the economy (≈energy) growth is more or less balanced by environmental degradation. If being focused on electricity production only - all countries are preparing a long-term energy plan for 2050 based on their renewable energy potential. Nowadays, there are several carbon-neutral energy sources available, including hydro, solar, wind, geothermal, and nuclear energy. All of these sources have own pros and cons and usage limitations. This thesis deals with base research in nuclear topics. Nuclear energy might be a part of the possible solution for covering the base load with no direct emission of CO_2. Its life-cycle emission is similar to renewable energy sources. Existing nuclear reactors are the most convenient for countries with low renewable sources potential especially. Although nuclear energy belongs to the most safety energy sources (the lowest „death per TWh“ ratio [5]), the public opinion is very fragile due to several serious nuclear accidents and radiation incidents. Despite public opinion, the problems are mostly high cost and long-term construction with often delays. If humankind expects that some carbon-free technology revolution may arise in further years, it is very hard to make a long-term energy plan for any country. Moreover, it is politically unpopular to take a considerable risk of making a long-term decision with a enormous cost. Existing newest reactors of III^+ generation represent an investment of about 60 years, plus at least a decade of paperwork and construction. The evolution of nuclear energy is expected by small modular reactor (SMR), smaller reactor units with advanced technology, compact size, and lower cost. Other cons are the future decommissioning due to radiation (which already calculated in life-cycle emission) and mostly discussed long-term radioactive spent fuel.

There are conservative plans of long-term storage of SNF, however, there is a possibility of reprocessing, and more challenging ones - the transmutation of a long-lived radioisotopes. This technology of transmutation is able to „convert“ long-lived and problematic isotopes (usually very toxic) to a short-lived one, even with releasing some extra energy able to use for potential customers (electricity generation). This dissertation deals with the base research in the frame of ADS, chiefly focused on various experimental target heat generation.

Chapter 2

Nuclear energy

The nuclear energy fascinates researchers and technical audience especially due to its high energy density. The nuclear fission reaction releases roughly 200 MeV per one fission. Thus, if all ^{235}U atoms in one kg of pure ^{235}U are fission, the energy density is about six orders of magnitude greater than combustion of hydrogen. Moreover, hydrogen combustion has not been commercially usable as a fuel yet. Humankind still burns fossil fuels. Ordinary fossil fuels have about three times lower energy density than hydrogen, and moreover its combustion releases a large amount of dangerous GHG. Its mining and further processes are widely devastating nature. Magnitude of released energy by combustion is basically in the same order with the energy released by digestion of food in the organism[1]. Energy density is a simple answer to all questions about so-called „nuclear madness“ during the middle of the last century.

Although nowadays technologies do not allow to fission any fissile mass fully, the nuclear fuel energy density is still enormous[2] in comparison with combustion. As the nuclear fuel is a very concentrated source of energy, it is very convenient for fuel transport and low storage capacity requirement, which allows to ensure the energy security of a country for several years.

2.1 Future expectations of NPP

Future of nuclear power production depends on several factors. Energy mix of each country is one of the most important geo-politic decision. It depends on the country location and environment. Flat countries can not count on water energy as well as less windy countries do not support wind power turbines. Countries closer to the equator have a better condition for photovoltaic power plants, but if they have an enormous site of gas in their territory, the motivation to build up renewable sources is suppressed. Hopefully, there are political agreements based on climate protection and carbon dioxide emissions reduction. However, there are several strategies of carbon dioxide reduction, but there is one which all signatories of Paris Agreement agree with - a coal reduction is mandatory.

In essence, it seems that nuclear energy will never supply more than 12 % of world electricity consumption. If look into the future forecast of the energy mix and consumption analysed by IAEA [7]. There are two scenarios. The final energy consumption was 427 EJ, of which 80.4 EJ was electricity (18.8 %) in 2019. Based on the expectation, about 592 EJ

[1] For pure lipids, protein and carbohydrates, it is 39, 23 and 17 MJ·kg^{-1} respectively [6].

[2] For example, if some Pressurized Light-Water Moderated and Cooled Reactor (PWR) have burn-up about 50 GWd·t$_{\mathrm{HM}}^{-1}$, it means that energy released from one kg of uranium is roughly 4.3 TJ·kg^{-1}.

will be consumed in 2050, of which 161 EJ (27.2 %) will be electricity. The world nuclear electricity production was 2,657 TWh in 2019. Based on the low case scenario, it should be 2,929 TWh in 2050, which represents about 5.7 % of totally produced electricity. Based on the high case scenario, it is 11.2 % of totally produced electricity. Present nuclear power capacity 392 GW_e should decrease to 363 GW_e (low case) or increase up to 715 GW_e (high case). Analysts expect the real scenario somewhere between these two extremes.

The question is what these results mean for the future of nuclear energy. It is expected that the nuclear reactor design will go through a revolution. Smaller mass-produced economical units with high passive safety, so-called SMR presented nowadays, should be a way. List of the SMR in research (Table 1.) [8] and all updated information find [8]. Moreover, there is a Generation IV of nuclear reactors. It is a group of six reactor designs which were selected by a special commission in 2001. It is Gas-cooled Fast Reactor (GFR), Lead-cooled fast reactor (LFR), Molten Salt Reactor (MSR), Super Critical Water Reactor (SCWR), Sodium-cooled fast reactor (SFR), and Very-high-temperature reactor (VHTR). The main positive aspects of these chosen are - proliferation resistance, waste minimisation, higher efficiency, and higher safety. Nuclear research worldwide is focused on these reactors.

There are some negative aspects of the current NPP - the spent fuel and its storage. This topic is discussed in another section, just to be briefly mentioned, it is one of the most problematic parts (if nuclear energy should be labelled as „green source“). As well, it is long-term lack of uranium. Both of these problems could be solved by the transmutation process, which is going to be discussed in the following chapter.

2.2 Sub-critical Accelerator-Driven Systems

Accelerator-Driven Systems (ADS) [9] are studied for the last three decades, mostly due to seeking a facility producing high energy neutrons able to breed fissile material for peaceful usage. These fast neutrons are simply able to decrease the toxicity and radioactivity of spent nuclear fuel. There were two main groups dealing with ADS technology during 1990'. The first project was led by C. Bowman in Los Alamos National Laboratory [10]. The project Accelerator Transmutation of Waste planned to use about 250 mA proton beam current with energy about 1.6 GeV. The second project was carried out in CERN by C. Rubbia [11]. Unlike the previous one, this one was not dealing with nuclear fuel transmutation, but rather deals with breeding fissile material by fast neutrons. Its name was The Accelerator Driven Energy Production project, also called as Energy Amplifier. The project was expected to use 1 GeV proton beam of 12.5 mA current. The transmutation is the key.

Finally, there are two main challenges of transmutation[3] in the nuclear energy sector. Ability to breed the fissile fuel, such as fertile ^{232}Th or ^{238}U, and decreasing spent nuclear fuel toxicity and radioactivity of its long-lived radioisotopes. Breeding of fissile isotopes is described by the following equation.

$$^{232}Th \; + \; n \; \rightarrow \; ^{233}Th \; \xrightarrow[22.3m]{\beta^-} \; ^{233}Pa \; \xrightarrow[26.97d]{\beta^-} \; ^{233}U$$

$$^{238}U \; + \; n \; \rightarrow \; ^{239}U \; \xrightarrow[23.45m]{\beta^-} \; ^{239}Np \; \xrightarrow[2.35d]{\beta^-} \; ^{239}Pu$$

[3]Transmutation is a process when the number of neutrons or protons in a nucleus is changed. The physical properties, such as half-life, activity, and radiation energy, are changed. The new nucleus is the same element, but different isotope. On the other hand, if the number of protons is changed, another nucleus arises with another charge, as well as the atomic number. In this case, the chemical properties are changed.

This process can not be widely achieved in nowadays commercial reactors due to the low probability of neutron capture, in detail discussed in [12] p.5-13, or [13] p.24-28.

The long-term radiotoxicity of the SNF is another topic, however it may be achieved by similar techniques. The spend fuel composition depends on reactor type, fuel enrichment, and its burn-up[4] [14]. In the case of PWR with a burn-up about 50 GWd·t$_{\mathrm{HM}}^{-1}$, the inventory of the spent fuel is about 93.4 % uranium (where ^{235}U represented by 0.8 %), 5.2 % fission products, 1.2 % plutonium, and 0.2 % minor transuranic elements (neptunium, americium, and curium) [15].

Radioactive waste is produced by many radiation applications, such as electricity production, or sectors such as health, food and agriculture, industry, and the environment. Radioactive waste is a disposal based on the level of radioactivity, globally divided into very low level waste (VLLW), low level waste (LLW), intermediate level waste (ILW) and high level waste (HLW). The SNF belongs to the last mentioned level and its disposal has very strict conditions. Due to its long-lasting radioactivity, toxicity, and internal heating, it must be specially encapsulated into an engineered multi-barrier storage system. This kind of SNF repository was already built in Onkalo [16], Finland. Therefore, the long-term storage is one of the possible solutions, however it does not utilise the SNF potential.
The other more effective one is the transmutation of long-lived radioisotopes which decrease the storage duration, in detail described in [13], p.9. Moreover, it opens great potential to use the fuel much more effectively. Generally, the whole idea is called P&T (Partitioning and Transmutation).

Transmutation of problematic isotopes may be achieved by two possible nuclear reactions - neutron fission or neutron capture. For long-lived acrfull FP is available only the neutron capture and due to its low reaction cross-section it requires a suitable (rather thermalised) neutron spectrum or (and) high neutron flux. However, the duration of the transmutation process still takes a long time. The actinide transmutation requires rather fast neutron spectra with even higher neutron flux, due to the fission reaction cross-sections are in a similar range for all actinides, and moreover the neutron capture CS is much lower (does not produce problematic higher actinides, such as Cm or Cf) . Since a very high neutron flux required, the fast reactor is not sufficient (the releasing heat is proportional to neutron flux production → cooling limits). For this reason, the spallation reaction is much more suitable for high neutron flux production.

2.2.1 Spallation reaction and ADS summary

Spallation reaction occurs across many science disciplines such as astrophysics, radiotherapy, radio-biology, geophysics, and all works dealing with accelerators. Despite this fact, there is no generally accepted definition of this term [17]. In cosmic ray physics it is referred as „fragmentation“. The verb „to spall“, means to chip with a hammer [18] or more modern - to break into smaller pieces, especially in preparation for sorting [19], anyway the verb dates from the mid 18$^{\mathrm{th}}$ century [19]. Spallation refers to nonelastic nuclear reactions that occur when energetic particles, for example, protons, neutrons, or pions interact with an atomic nucleus [17]. The reaction can only occur if one of the reaction partners is a complex nucleus. The received energy increases the interaction energy between nucleons in the nu-

[4]Burn-up is the fuel utilisation - it describes the amount of energy extracted from the fuel mass, usually formulated in unit GWd·t$_{\mathrm{HM}}^{-1}$, where *HM* means heavy metal, which corresponds to the mass of the fuel. The energy unit GWd is equal to 86.4 TJ, so the 1 GWd·t$_{\mathrm{HM}}^{-1}$ $\approx$ 86.4 GJ·kg$_{\mathrm{HM}}^{-1}$.

cleus. Therefore, the spallation or spallation reaction is a nucleon–nucleus or pion–nucleus or nucleus–nucleus reaction, in which the energy of the projectile is larger than a tenth of MeV per atomic weight. Actually, it is not certain that spallation occurs if the described conditions are met, other reactions may occur. The spallation is a complex sequence of nuclear and atomic interactions.

There is no clear separation barrier of spallation from the lower energy nuclear reactions. There are several non-exact versions of spallation reaction descriptions, of which the shortest one is: „Spallation is a nonelastic nuclear interaction induced by a high-energy particle $\geq$50 MeV producing numerous secondary particles“ [17]. In essence, it is based on the projectile ability to interact directly with the nucleons of the nucleus. This ability depends on the De Broglie wavelength, which has to be less than the size of nucleus. For example, 1 GeV proton has λ=9·10^{-14} cm, or 150 MeV has λ=2.3·10^{-13} cm, but on the other hand smaller energies as 10 MeV has λ=9·10^{-12} cm, which is actually the size of heavier nucleus.

Components of ADS

One of the biggest advantages of the ADS is their safety due to subcriticality. It is a sort of hybrid reactor which requires an external neutron source to sustain fission reactions in the sub-critical fuel assembly. When the external source is switched off, the fission chain reaction can not continue. This source of neutrons may be carried out in various ways. This thesis deals only with a spallation neutron source by employing an accelerator with high current, typically in units of mA, and high particle energy, roughly 1 GeV. The target has to be a heavy metal, such as lead, tungsten, wolfram, or others. More suitable seems to be liquid metals such as tungsten, liquid lead, or lead-bismuth eutectic, due to better heat extraction and its operation possibilities at higher temperatures which allows wider utilisation.

The most important parameter of the ADS concept is its energy gain, usually marked as G, and the neutron production number, which is crucial for the design. The number of generated neutrons per incident particle (and final neutron spectrum) defines the capability of fissile material breeding and the capability of nuclear waste transmutation. Due to the high cost of a demo unit, projects are usually designed with multipurpose utilisation, including medicine, material science, geological science, archaeology & heritage conservation, and globally fast neutron applications.

Accelerator of ADS should be in the range of current roughly 10 mA for a demo unit and further about 20→100 mA for the commercial power plant, in case of considering the most economical 1 GeV proton beam. There are several accelerator variants, however, the most economical is a cyclotron design. Unfortunately, the cyclotron design is limited by either energy so the intensity. More variables are linear accelerators, which are mostly used in ADS. Moreover, this accelerator type is usually more economical, primarily in the case the accelerator facility consists of more than one accelerator and the expected particle energy is achieved by acceleration step by step up to reaching the required energy value.

Target of ADS consists of heavy metal material due to the fact, that higher mass number of the target increases the neutron yield of the spallation reaction. As mentioned, the heat generation inside of the target may cause problems with deposited heat transferring to cool the target down. Charged particles (projectiles) lose their kinetic energy passing through matter by excitation of bound electrons and ionisation. The heat is generated chiefly by Coulomb scattering and ionisation loss as the projectile goes through the target. **This dissertation thesis deals with experimental research of thick targets suitable for ADS.**

2.2.2 Current research of ADS

There are dozens of research focused on ADS technologies. History of this research is very well summarised in the previous colleagues works [20] (Czech) and [13] (English). Ongoing projects and their potentials are well discussed by World Nuclear Association in [21] and by IAEA in a summary publication [22]. The ADS are also discussed in connection with molten salt reactors and thorium energy (for more information see [23] on p.495-521). As the ADS research is not much dynamic, it has been decided to only shortly discuss the most important ongoing projects. Two of them are in Europe, one is in China.

EES (European Spallation Source) [24] in Lund, Sweden, is not actually focused on ADS, but it is an essential project for the future of ADS research. It is already in construction which uses spallation source for many research activities. It is based on a linear accelerator with maximum energy 2 GeV, average current 62.5 mA, frequency 14 Hz, and peak power 125 MW (average 5 MW). The spallation source is made of a 4 t rotating tungsten target (diameter of 2.6 m) which is cooled by liquid helium (-271 °C). Its neutron production rate is about 80 fast neutrons per incident particle. This project does not directly deal with ADS, its neutron research deals with all branches like physics, chemistry, geology, biology, and medicine. However, it is expected that reached knowledge helps in all topics dealing with spallation targets, so the ADS.

MYRRHA project at SKC·CEN [25] in Mol, Belgium, is focused on the transmutation of spent nuclear fuel. There is a synergy with pharmaceutic industry and besides the research of transmutation, it will produce medical radioisotopes.
The financial support of the project, or rather the first phase of the project, has been signed in 2018. It consists of 100 MeV accelerator (0.5 mA) which will be extended to 600 MeV in the second phase by 400 m LINAC. The current of the LINAC should be 4 mA which goes to the reactor. The pool type reactor will be cooled by 7,800 tons of lead-bismuth eutectic [25]. The motivation of MYRRHA project is to revive the idea of the long-lived radioisotope transmutation into much shorter living ones. Present technologies are able to decrease the radioactivity of SNF from 300,000 years to about 10,000 years by reprocessing (so-called MOX fuel). Transmutated SNF reaches similar radioactivity after about 300 years of storage [25]. The last phase of MYRRHA should be finished until 2033.

ADANES complex project [26] at IMP in Lanzhou, China is dealing with ADS Burner (ADB) and a system of Accelerator Driven Recycle Used Fuel (ADRUF). The ADB will achieve transmutation of long-lived radioisotopes, fuel breeding, and energy production. At the same time, ADRUF prepares the recycled fuel. The project is similarly divided into several phases but should be finished already in 2030. The first phase was dealing with breakthroughs of key technologies related to ADB and ADRUF (2011-2016). In the second stage between 2018-2024, the construction starts of the high-power ADB research facility, China Initiative Accelerator Driven System (CiADS) and an ADRUF with a hot cell and a compact neutron source. The CiADS consists of a 2.5 MW superconducting proton LINAC with 500 MeV and 5 mA, a liquid LBE cooled fast reactor with 10 MW_t [26].

ADS research at JINR in Dubna
The early first research of spallation reaction or ADS began during the 1970s, however, intense research in DLNP was started in 1990s. Based on this activity later arose a collaboration E&T RAW. Since the 90's there is a continuous research dealing with various topics - the neutron production studies; neutron transport; transmutation of actinides (in n spectrum moderatednot); energy gain studies; or studies of transport code benchmark.

Previous experimental targets

The ADS research group studied several experimental setups in previous years, very shortly that were studied the following targets: the LEAD block target, GAMMA-2, GAMMA-3, and The Energy plus Transmutation target. Its description is discussed in p.53-55 of L. Závorka thesis [13]. Those targets were irradiated at all previously mentioned accelerators, based on the year of irradiation. The targets of which this thesis deals with are described in following.

Phasotron accelerator

All experimental research of this thesis was performed at Phasotron accelerator facility which consists of a proton accelerator with several channels for medical or experimental utilisation. It provides usually 1 μA (3.2 μA maximum) proton beam with energy of 660 MeV without an ability of energy tuning. However, it allows to use a beam with energy 200 MeV for direct irradiation inside of Phasotron - without using any extraction channel. The accelerator diameter is about 5 m, mass about 7 000 t and magnetic field in the range of 1.2-1.6 T. The electricity power consumption of the accelerator is about 1.5 MW and the same for the beam extraction facility (the total power consumption is 3 MW). The experimental channel in the experimental hall has been used for all performed experiments. Due to this channel setting, the beam parameters are diametrically different to the experimental channel beam extraction values. The irradiation channel beam parameters decrease a lot, the current up to $\approx$ 1-3 % of the accelerator nominal values and the beam geometry (gausian FWHM) increase approximately 4 times. These information were extracted from [20] and discussion with the accelerator manager.

TA QUINTA The abbreviation QUINTA is based on its description: quasi-infinite uranium target. It consist of 298 uranium cylinders ($^{\mathrm{nat}}$U) located in five hexagonal sections. While the first section has a beam window (cylindrical air hole) and contains only 54 cylinders, each other section is equivalently fully filled and contains 61 cylinders per section. The cylinder with diameter 36 mm and length 104 mm weight about 1.7 kg. In total it consist of 512 kg $^{\mathrm{nat}}$U.

BURAN

The BURAN is a sub-critical cylindrical blanket with length of 1 m and diameter of 1.2 m consisted of 20 t of depleted uranium (0.3 % of ^{235}U), covered by 10 cm of steel cladding. BURAN has 72 measuring channels which may be equipped by activation samples or any other measuring device (such as thermocouples - earlier planned to be apart of this PhD research). In the centre of BURAN, there is a hole of 20 cm in diameter where a cylindrical spallation target with a shape of 19 cm in diameter and length of up to 1 m is supposed to be install. By reason of better neutron flux distribution, it is discussed to use a combination of several target materials in a cylindrical shape with length of 5$\rightarrow$10 cm (experimentally studied by *exp12* and *exp13*). Target description, visualisation, and experimental results are shown and widely discussed in chapter 5.1 for the LEAD target and in chapter 5.2 for the CARBON target. The BURAN is supposed to be an „infinite target“ with a small amount (about 15 %) of leaking neutrons (in comparison with 75 % of the QUINTA target, data based on P. Tichý MCNPX simulations [27]). Experiments with BURAN have been planned since 2019. Unfortunately, due to the combination of several complications, the experiments have not been performed yet (written in the end of 2020).

Chapter 3

Methodology

3.1 Temperature measurement and analysing methodology

There are many variants of how to measure the temperature. For several reasons, the small diameter thermocouples T were chosen. It consists of two metals, copper and constantan (an alloy of copper and nickel). The chosen thermocouples fulfil the requirement of the short response time due to the chosen wire with diameter of 0.51 mm. To ensure as accurate measurements as possible, the thermocouples are connected as a whole, without any cutting and connection.

Data acquisition was performed by the National Instrument (NI) hardware with employing the LabView [28] software (also from the NI). The measuring cards (A/D converter) NI9214 and NI9212 were chosen due to the best ration of accuracy/number of channels/-cost. Converters were input to chassis cDAQ9174, also from the NI (more information on the p.9).

Manufacturing of the thermocouples

One of the tasks was to measure 88 positions of the QUINTA target online. As the thermocouples needed to be used as a whole (for 22 m), about 2000 m of extended thermocouple wire was required, including some reserves. To reduce the cost, the thermocouples were self-made by using the thermocouples welder TL-WELD [29]. The low-cost thermocouple extension wire was purchased in the length of 300 m, cut into 22 m length and welded. The range of the measured temperature will be in range $T_s \rightarrow (T_s+\Delta T)$, where T_s=temperature of surrounded air, ΔT=temperature difference caused by target heating. The CJC must be taken into account. Based on the pilot experiment, the ΔT was expected to be around 10°C and surrounded air about 20°C. The most suitable thermocouples for this application are the thermocouples type T due to the highest accuracy, low impedance, and suitable measuring range with satisfied voltage gain. The thermocouples were specially calibrated by using linear approximation of derivative calibration equations from data sheets. The dissertation uses for this value term ΔV_{gain}, are widely discussed in PhD thesis.

Electronics & data collection in LabView

The most crucial part of this experimental research was the right choice of the electronics, chiefly the measuring card equipment. It must be as accurate as possible, since 1 μV is very roughly equal to 0.025 °C. The NI9212 and NI9214 fabricated by the National Instrument company were chosen for the thermocouples and NI9217 for RTDs measurement.

The data collection was realised by LabView [28] software. The earlier experiments were measured by using its DAQ (Data Acquisition & Analysis) assistant. It is a useful and easy to use tool, moreover it allows to set some basic parameters. Unfortunately, it does not allow to read cold junction compensation (CJC) data. Thermocouples were loaded as a voltage signal, without using internal calibration. For improving the measurement was prepared another code in LabView written by using DAQmx.

3.2 Simulation by MCNPX and ANSYS Fluent

The experimentally measured data were compared with simulation. The MCNPX simulation was calculated where the total heat deposition was estimated per chosen volume and per created mesh. The target volume was partitioned into cubes with the edge size of 2 mm and for each cell was calculated the relative heat deposition [MeV$cdot$cm^{-3}·proton^{-1}] This 3D heat source distribution was approximated by several equations as a 2D rotating heat source and defined as the specific heat source in ANSYS Fluent. That is the relative heat source distribution. The total number of interacting protons was estimated by gamma spectroscopy method of irradiated Al and Cu activation foils and finally this total proton number was recalculated over the irradiation time by using the relative monitoring of the proton beam by proportional camera. Since proton current over irradiation time is calculated, the heat power source can be defined by UDF of the ANSYS Fluent.

Monte Carlo N-Particle Transport Code simulation

The experiments were simulated by MCNPX 2.7.0., with employing the data library ENDF [30], Intra Nuclear Cascade modeL INCL4 [31], and the ABLA fission-evaporation event generator [32]. Neutron and proton spectra were calculated for several experiments (only where the samples were measured by gamma spectrometry method). Most of the simulations in this thesis are mostly focused on the heat deposition determination. Each of the MCNPX simulations were fully performed by the author, except the QUINTA target, where the QUINTA geometry model took over and rebuilt from the research work of M. Suchopár [33].

Heat transfer simulation by ANSYS

In this thesis were used calculations in Transient Thermal program and Fluent, partly by using the Workbench environment. In the following pages will be described problems the author dealt with, and finally, the used methods to calculate the required results. There are many variables to estimate and many choices need to be done for each simulation. The most problematic part was setting the variables for natural convection measurement and primarily to define the heat source which proportionally depended on the proton beam current and its distribution is spread through the whole target. It is widely described in the full version of PhD thesis.

Chapter 4

Experimental research - QUINTA

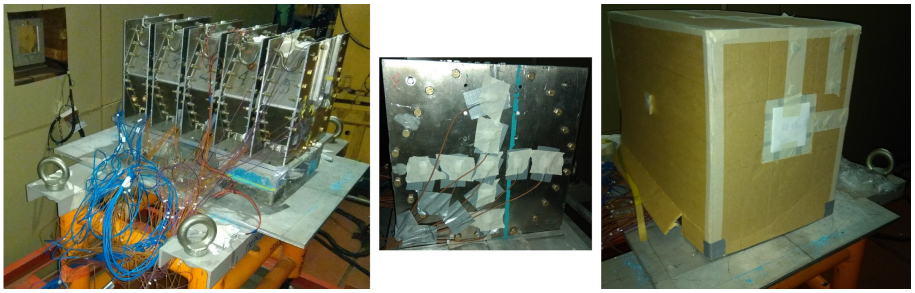

Figure 4.1: On the left side is shown the whole TA QUINTA without shielding with already fixed thermocouples. The thermocouples were fixed directly to aluminium cover for front and back side of each section by highly adhesive tape. On the right side, there is pictured setup just before the experiment. The QUINTA was covered by cardboard box to create a thermal boundary where convection is limited.

4.1 ΔT measurement of TA QUINTA heat generation

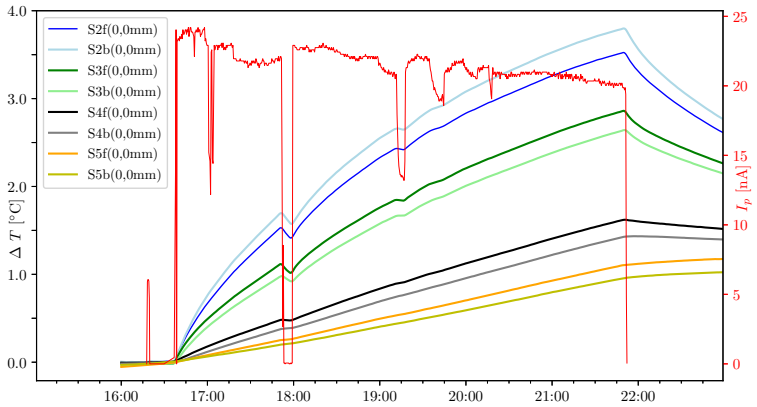

Figure 4.2: TA QUINTA temperature measurement without shielding in the centre of each section. This chart shows the problematic combination of the direct heating process and the surface cooling. The most of the heat is released in the second section, but either, the second section is cooled the most from the front side due to a hole in the first section. By this reason, the front side of the second section is cooler than the back side. If first section without hole, hypothetically, the front side of all displayed section would be warmer than the back side.

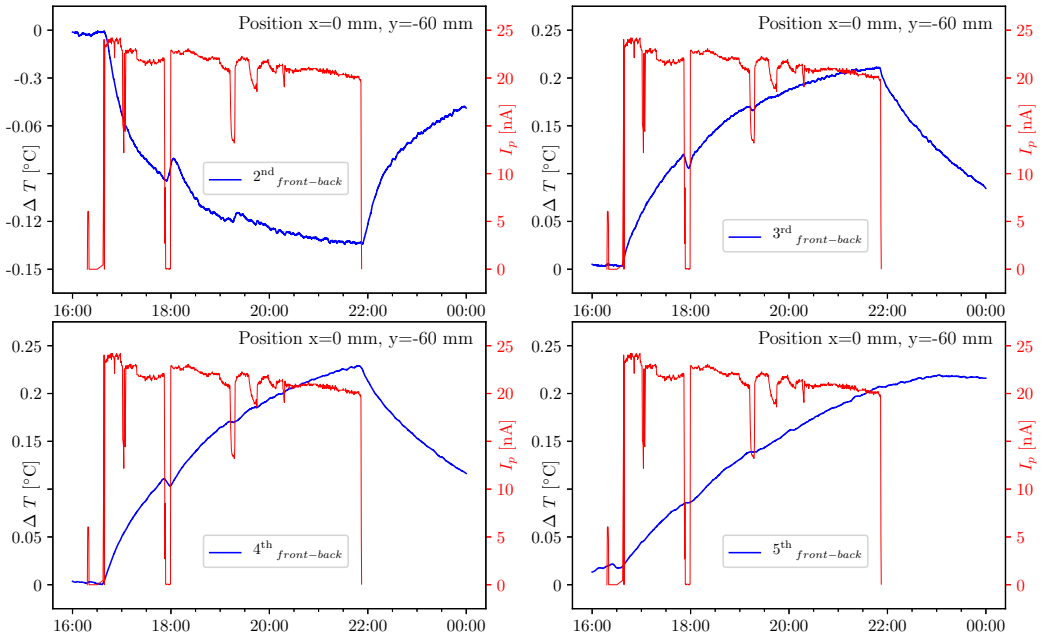

Figure 4.3: TA QUINTA temperature measurement without shielding with front-back differences shown. This figure describes the phenomenon of the different cooling of each section. Basically for each section, the front side should be warmer than the back one, due to more reactions appear there. Even more significant contributor of the accumulated heat loss is missing heat reflection of the first section, due to only 17 mm air gap between the sections. In further it is already mentioned extra access of the cooler air taking away the heat by natural convection.

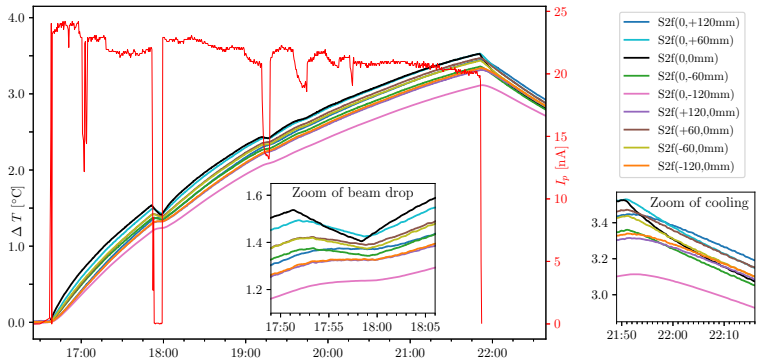

Figure 4.4: TA QUINTA temperature measurement without shielding, front side of the 2nd section. All measured position displayed. The chart consist of two additional zoomed windows. Firstly, it is the first beam drop, and in further below the legend, it is the end of irradiation (only cooling process and heat transfer occurs there without any direct heating).

4.2 MCNPX simulation of TA QUINTA without shielding

There were two methods of heat deposition calculation. The first method uses the basic heat deposition tally without meshing. Each cylinder is defined as a tally volume and separately calculated for each particle reaction contribution. It allows to separate the heat deposition of the target (uranium cylinders with cladding, in total 298 pcs) and the heat deposition released by the Al construction of the QUINTA target.
The second method calculate the fine target mesh deposition tally per each particle contributing to heat deposition. It is very suitable for visualisation purposes and for better understanding the target behaviour. The last mesh definition in this code (rows 301-306), was used for controlling purposes. It consists of only one cell, which contains the whole QUINTA volume (with extra 1 mm for each direction). It calculates the average value of this volume relative heat deposition density.

The MCNPX code and its utilisation have been already discussed (p.10), as well the visualisation methods by Python Seaborn. In these results will be shown only the final heatmap charts, cylinders heating visualisation and tables with important data. Usually, it is expected and appropriate, to share the MCNPX input file for controlling purposes. The Python code visualisation was very similar to that which used for other targets plotting. To make this dissertation more „open-access“, all MCNPX results (output files) are enclosed in full version of PhD thesis, or rather uploaded to Google Disk accessible for all BUT students or employees.

The first method results:
The relative heat deposition of each cylinder was simulated for proton, neutron, photon, pion reactions, and finally their summary per each section. Unfortunately, the visualisation of cylinder heating is tricky to be clear. The best way is to use the heatmap (which already used even better in further mesh). The summary per each section is shown in the following 2D chart with added total ratio visualisation by pie chart.

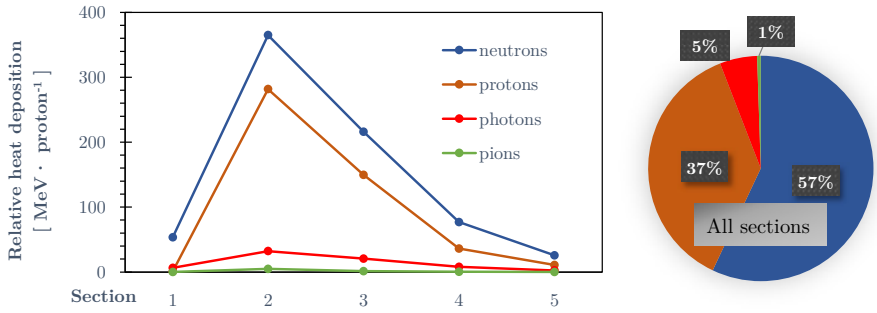

Figure 4.5: This chart shows the relative heating of the uranium cylinders with Al cladding per individual sections. Four sources of the heat are separated, based on the projectile of the heating reaction (protons, neutrons, photons, and pions).

The second method results:

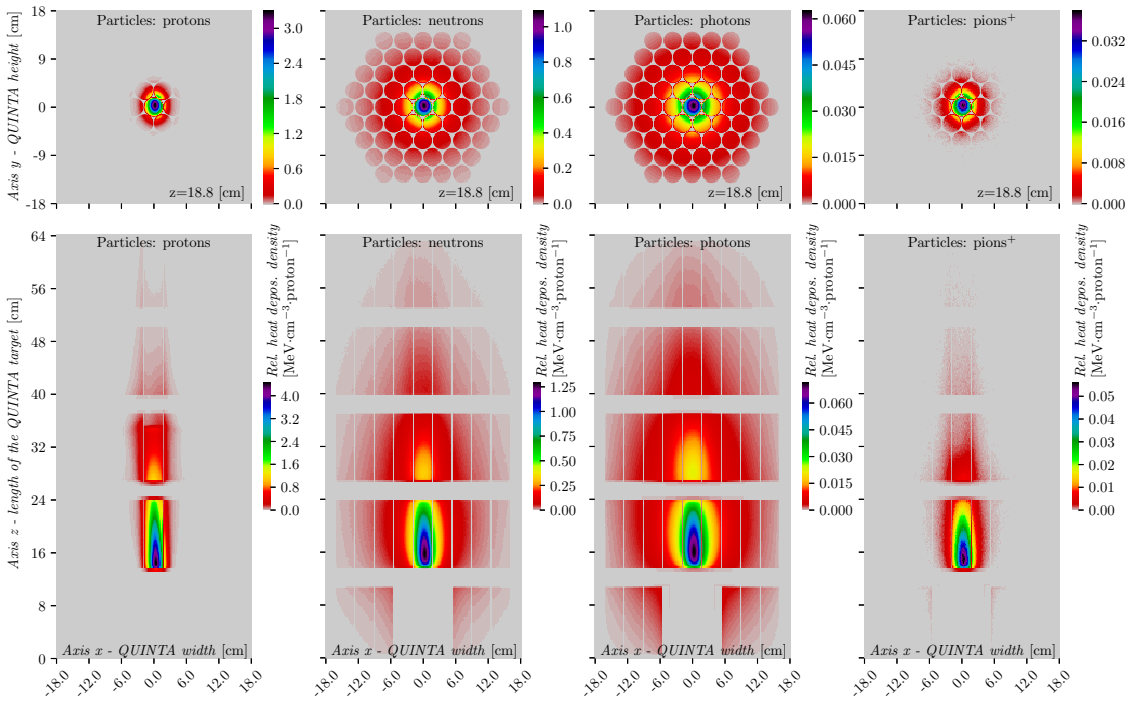

Figure 4.6: TA QUINTA - MCNPX simulation of relative heat deposition density separated into individual particles which reactions contribute on heat deposition. Each chart has unique maximum of the heatmap bar to describe the heat generation distribution per each participating particle in detail scale. Upper part shows xy planes, and the xz planes are displayed at the bottom. The proton reaction causes very concentrated heating due to ionisation loses and globally phenomenon described in section 2.2.1, as the secondary hadrons continues in direction of the primary particle for intra-nuclear cascade of spallation reaction. Neutrons are spread randomly in all directions. The neutron heating is concentrated the most in the centre due to the highest neutron flux concentration (the most of reactions), but it is much better distributed to surrounded target parts. The heat generated by neutron reactions (mostly uranium fission) is radially decreasing up to the target border. The gamma heating is well distributed through the target but it has much smaller total heat contribution. Finally, the pion heating reactions. They are similarly spread as the proton heating reactions due to their origin from the spallation reaction, in contrast with the proton reaction heating, the pion reactions contribution is merely negligible.

4.3 The results discussion

Experimental measurement:
Relative temperature measurement reflects changes of the target internal energy state, so it allows to observe the relative heat changes. These heat changes are caused primarily by three phenomenons. The first one, causing the heat increase, directs heating by nuclear reactions in the volume of the measured surface (this one is required to be monitored). The others two deal with the heat transfer - increasing of the internal energy state by the heat accumulation from warmed parts, and decreasing by releasing accumulated heat from the surface to surrounding parts. While the heat transfer from target direct heating is transferred in volume mostly by conduction, the surface is cooled chiefly by convection and radiation and the amount of transferred heat depends on the surrounding objects internal energy state. They can accumulate the transferred heat or reflect it (if radiation occurs). It is tricky to separate these three phenomenons by simple temperature change measurements.

For this reason, there is shown chart (Fig. 4.4) with very important temperature decreasing monitoring (when outage, the beam current is changed, or the irradiation ends). It allows to separate the heat transfer from direct heating. The target direct heating is caused by the proton flux occurrence, so its outage or changes affect the heat deposition directly. Due to good conduction, this phenomenon is able to observe where the direct heating is a major contributor of internal energy changes (sharp temperature changes). On the other hand, if the internal heat changes are chiefly caused by heat transfer, the beam outage is not affecting the changes of internal energy $\rightarrow$ the temperature changes are very smoothly with some time delay which depends on the heat transfer rapidity.

To summary, the most directly heated parts are in the centre cylinders of each section, see the black line as sharply decreasing since the beam drop (in Fig. 4.4). It is chiefly caused by proton heating. Similar sharp trends with lower slope are shown in the positions $\pm$60 mm - as vertically so horizontally, mostly in the second and third section. In essence, the direct heating of the central target's uranium cylinder depends on the beam position and its flux. It is suitable to expect that the upper parts will be heated by heat transfer of the warmer central part by natural convection, but of course all of the three heat transfer processes occur. Temperature measurement is chiefly affected by the proton beam window, which causes the quantity and rapidity increasing of the front 2^{nd} section cooling.

MCNPX simulation:
The MCNPX simulation allows to simulate the heat deposition caused by various nuclear reactions. Particles whose reactions caused the chief portion of direct target heating were neutrons and protons. Besides these two, there were simulated minor contributor reactions caused by photons (so-called gamma heating) and pions^{+}. To compare the total heat deposition by each contribution particle reaction, most of the heat is released by neutron reactions (mostly fission), about 57 %, followed by proton reactions which contribute by about 37 % and finally, the gamma heating contributes only 5 % and pions merely less than 1 %. The summary chart is shown in Fig. 4.5.

Chapter 5

Other targets research

In the frame of this dissertation, another two targets were researched besides the QUINTA target. These targets were irradiated and studied by several methods by reason to prepare the most suitable target for sub-critical blanket BURAN, described in section 2.2.2. Prolonged targets of lead and carbon were constructed and finally irradiated by 660 MeV protons at Phasotron irradiation facility. These materials were chosen for detail study due to their varied neutron spectra. The LEAD target produces dozens of fast neutrons, while the CARBON target produces fewer neutrons at much higher energies. Based on the simulation, the lead material stops the 660 MeV protons in a distance of 30.7 cm (without air gap) and for the carbon material it is in distance of 112.5 cm. By a combination of these two materials can be prepared the most suitable target for future BURAN experiments.

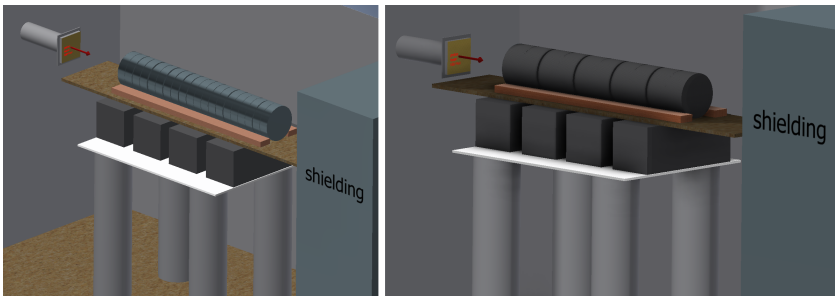

Figure 5.1: Model of the LEAD (left) and the CARBON (right) target irradiation.

5.1 LEAD target

The LEAD target consists of twenty cylinders, each with diameter 19 cm and length 5.2 cm. There was a problem with the lead material that the geometry is not easy to machine, so the cylinder geometry has 1 mm tolerance, however, the cylinders contain small fragments on the surface causing roughness up to 2 mm. Between each two neighbour cylinders, there was an air gap for measuring purposes. If only thermocouple measurement was involved, the air gap was minimal (primarily caused by rough geometry). After 2^{nd}, 4^{th}, 6^{th} and 8^{th} cylinder, there were a larger air gaps where copper and lead activation foils are installed. Mass density of the lead was ρ_{Pb}=11.35 g·cm^{-3}. The total target length was 108.1 cm. It was consisted of 104 cm of the lead and 4.1 cm of several air gaps. In principle, only first 6 cylinders significantly interact with protons. The target was irradiated by 660 MeV protons for 265 min excluding several of the planned beam pauses (purpose of cooling observation).

5.1.1 Temperature measurement of the LEAD target

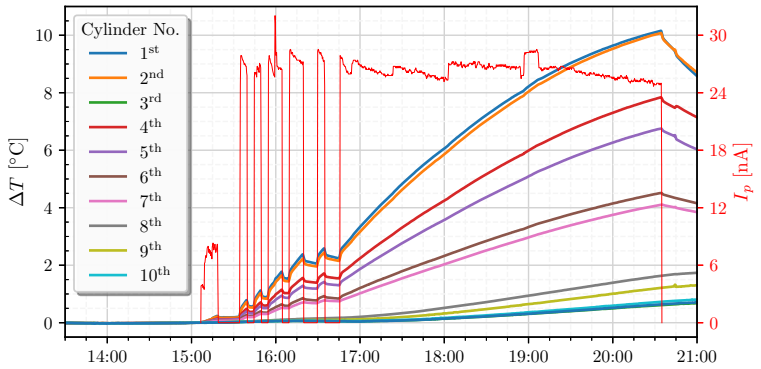

Figure 5.2: Thermocouples temperature measurement of the LEAD target (*exp13*). The temperature was measured by thermocouples on back-side of each cylinder. Only front 6 cylinders are significantly contributing on heat generation (discussed on page 17). This phenomenon is confirmed by experimental temperature measurement. If the cylinder generates significant heat, the increasing temperature should correspond with the proton beam occurrence. On the other hand, beam outage should causes the target cooling → temperature should decrease when beam absence. If these conditions are visible by ΔT measurement, the measured temperature increase is caused by any of the heat deposition reactions. If the cylinder temperature is increasing very slowly and does not respond to beam occurrence, the increased temperature is probably caused by heat transfer from surrounding parts (cylinders heated by particle reactions). It is represented by cylinders 7-10. Other cylinders are not displayed for better clarity (negligible ΔT).

5.1.2 Simulation of the LEAD target by MCNPX and ANSYS Fluent

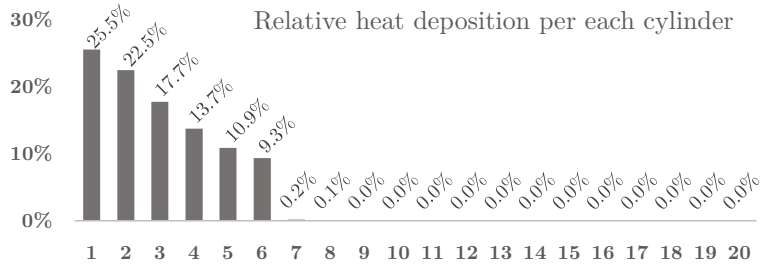

Figure 5.3: Relative total heat deposition per each cylinder of the LEAD target (proton, neutron, photon and pion$^+$ reactions included). Axis x represents the number of cylinder, axis y represent relative heat deposition of each cylinder to the total target heat deposition. The heat deposition mesh tally was calculated for the whole volume, however due to its larger size it is not shown in shorten version. By its results was approximated the heat power source.

Fluent simulation results

The fluid temperature (target cooling by natural convection) was monitored over the irradiation time. The solution animations were created and are available on YouTube dissertation channel. The 3D static visualisations of the ANSYS Fluent simulation are shown in Fig. 5.4

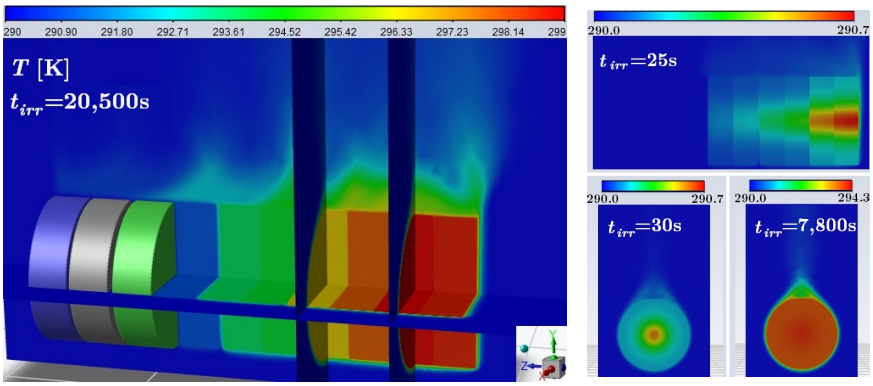

Figure 5.4: Fluent simulation results of the LEAD target temperature distribution in various irradiation time and various planes. On the left side is shown the 3D temperature visualisation in irradiation time 20,500 s. The solid of cylinders 8,9,10 is visualised. The right side of the figure shows *yz* plane on the top and two *xy* planes at bottom part. The irradiation times are listed in the respective figure screen.

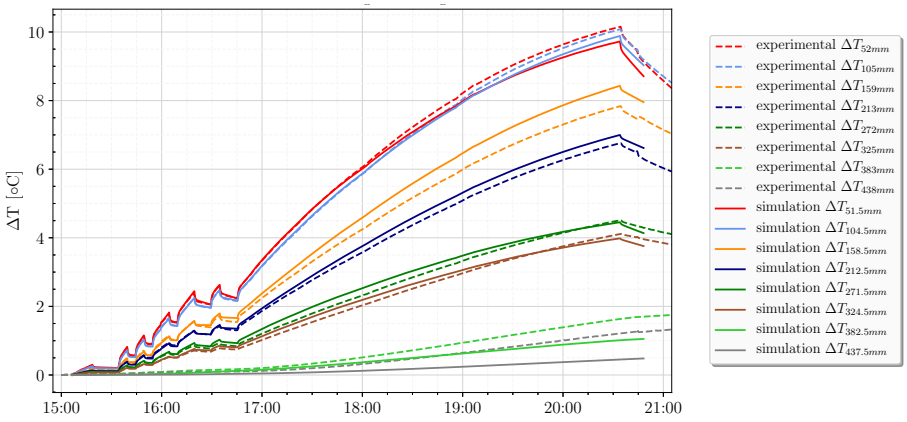

Figure 5.5: Comparison of the ΔT for ANSYS Fluent simulation and experimentally measured data - final results. The achieved results are discussed in following section.

5.1.3 Results discussion - LEAD target

The LEAD target was irradiated by 660 MeV protons for 5 hours including several irradiation pauses for target cooling monitoring and for monitoring heat transfer through the thermal insulation. The temperature measurement reflects the proton flux without extra delay. Such a tiny proton beam current changes as 0.6 nA (from 2.6→3.2 nA) lasting less than 20 s was reliably detected by TC probes. Temperature changes were measured in the

back-side surface centre of each Pb cylinder. Due to negligible ΔT changes of more distant cylinders, only the first 10 cylinders are shown in charts. About 99.7 % of the heat was released in the 30.7 cm of the lead. In summary, 95.12 % of the total target heat was generated by protons reaction, 3.03 % by photons (gamma heating), 1.17 % by pion^{+}, and about 0.68 % of the total heat was generated by neutron reactions. The thermal power distribution in the cylindrical volume was calculated by MCNPX, approximated with a Python script by several equations, including its dynamic changes caused by proton current instability during the whole irradiation time. These equations were written in C language to User Defined Function (UDF) and used as a dynamic source definition for ANSYS Fluent heat transfer simulation. The current of the proton beam over the irradiation time was calculated based on relative current monitoring by gas-filled ionisation chambers, combined with the estimated total number of interacting protons acquired by the activation foil technique (Cu and Al foils evaluated). The frequency of the proton beam current monitoring is about 0.06 Hz.

The final comparison between the experimental data and simulation is shown in Fig. 5.5. The simulation fits very well the experimental measurement. The maximal simulation error is about 7.5 % for the third cylinder measurement. It is caused by several factors. On the surface of the target was fixed the experimental samples by paper tape and a cardboard construction was inserted between cylinders. It influences the heat transfer a lot. The construction parts which were holding the target are not simulated, as well as the ionisation chamber on the front side of the target. It changes the fluid cooling behaviour in the real experiment. The roughness of the Pb cylinder geometry and sharp surface fragments cause the uncertainty of the volume for simulations in MCNPX and Fluent. Finally, there are ANSYS Fluent model uncertainties caused by the approximated heat source definition (uncertainty up to 5 %) and the mesh roughness in more distant parts. The ΔT measurement uncertainty also slightly contributes to the total experiment vs. simulation error.

The experiment of neutron flux monitoring shows very interesting results. The two geometrical similar probes of Ta and $^{\text{enr.}}$U materials were placed at similar neutron flux, covered by thermal insulation and its heating was monitored by very accurate TC measurement. The dependency of ΔT to proton beam current changes were monitoring. This measurement is very dependent on the thermal insulation quality, data acquisition setting, and surrounding fluid conditions. The direct heating can be determined due to several beam outages - heat transfer from the warmer target has a delay, and is suppressed by thermal insulation. By this measuring method is even visible (detectable) such a small proton current change as mentioned 600 pA. This method is suitable for short irradiation pulse monitoring. Tiny volume probes are very sensitive, however, the measurement sensitivity should be studied in laboratory conditions with unified neutron source utilisation. It was planned to compare the experimental results with the MCNPX simulation of the heat deposition and the neutron flux of the neutron leakage to discuss the sensitivity and accuracy of the measurement. Finally, it has been decided to publish these results directly in the prepared publication.

5.2 CARBON target

The CARBON target consists of ten cylinders, each with diameter 19 cm and length 10 cm. The air gap realised for measuring purposes (for the thermocouples measurement and activation foil installation) was about 1 cm thick, located after each even cylinder. Mass density of the carbon was ρ_c=1.8 g·cm^{-3}, based on the manufacturer data sheet. The total mass of the whole CARBON target was about 51 kg. The total target length was 104 cm (consisted of 10×100 mm of the carbon cylinders and 4×10 mm of air gap). Due to a low reaction cross-section of carbon, some particles are going through the target (the proton beam Bragg peak would be located in the carbon length of 112.5 cm, based on MCNPX simulation). The target was irradiated by 660 MeV protons for 277 min excluding several unplanned beam outages caused by beam instability, see the Fig. 5.7. Actually, the beam instability had a positive effect for the target cooling monitoring, to estimate the direct heating caused by beam occurrence, and finally, for the comparison of experimental vs. simulated dynamic data. The total experiment duration was about 336 min and the total number of incident protons was determined to $N_p = 2.40(19) \cdot 10^{15}$. The beam parameters were: $FWHM_x$=35.1 mm, $FWHM_y$=34.6 mm, x_0=-5.1 mm, y_0=-0.1 mm.

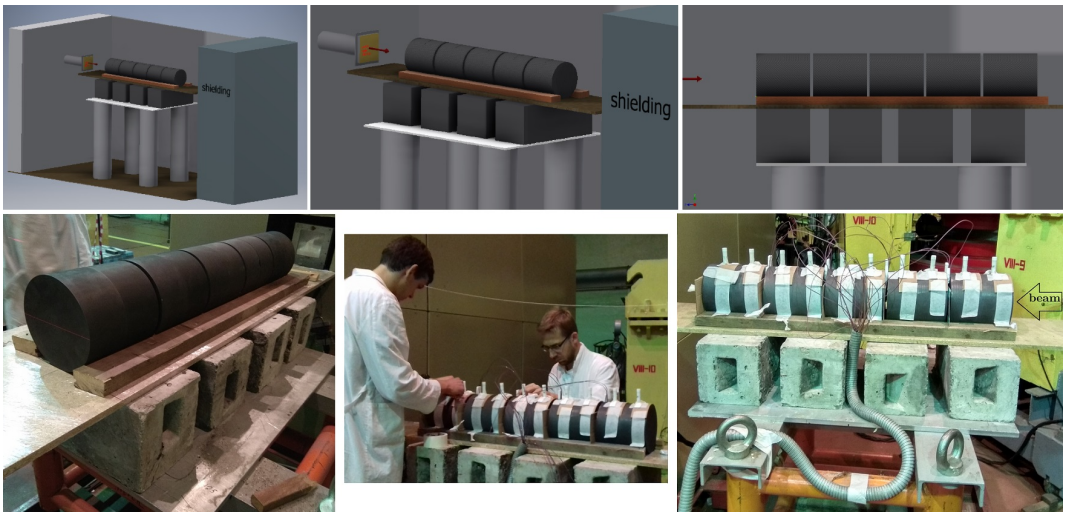

Figure 5.6: The 3D CAD model visualisation of the CARBON target is shown on the top of this figure. At the bottom part, there are real photographs from the experiment preparation. The final installation of the target is shown on the most left side, the thermocouples and activation foil installation by author (wearing glasses) and salt ampules samples by D. Král (black hair) is shown in the centre, and finally the CARBON target ready to be irradiated on the most right side (with the proton beam direction label).

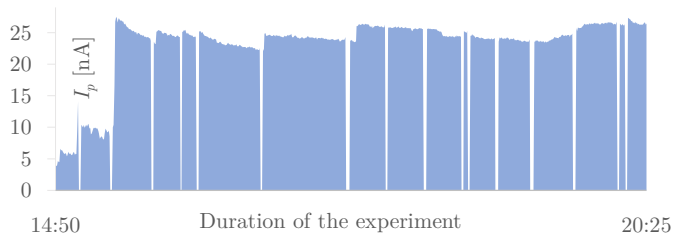

Figure 5.7: The proton beam current during the CARBON target irradiation.

5.2.1 Temperature measurement of the CARBON target

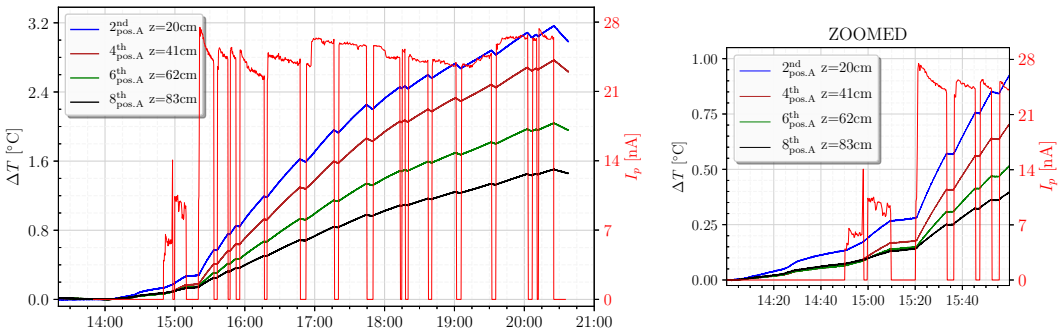

Figure 5.8: The main temperature measurement at the position „A“ of the CARBON target is displayed on the left axis y together with the proton beam current on the right $y2$ axis. Based on the temperature measurement results analysing it must be stated that the heat is distributed quite evenly, as in the radial direction, so along the target length. As the protons interact with the target along whole length, the temperature is uniformly and slowly decreasing along the target length. The maximum of measured temperature differences reaches about 3-time lower values in comparison with the LEAD target. It is caused mostly by lower proton interaction of carbon, therefore the Pb target releases the heat in much smaller volume, and generally there is different specific heat constant. Zoomed part of the experiment beginning is shown on the right side by reason to discuss the temperature measurement sensitivity of surrounded conditions. The experiment was prepared in advanced. The instruments were installed and the measurement was started about 24 hours before the experiment has begun, to get steady temperature of target and electronics. Unfortunately, one of our colleague was installing some instrument during 14:15-14:30 $\rightarrow$ T of the 2^{nd} pos. increased.

The thorium sample was installed inside of the CARBON target to compare the temperature of Th and temperature of the target. Based on the expectation, the Th sample reaches higher direct heat power density than the carbon material if the proton beam occurs (higher heating reaction cross-section). It was measured and analysed by very accurate technique and the results of the measurement are show in Fig. 5.9.

Finally, the linear regressions of each ΔT peaks are compared together and the median of all peaks is calculated per each position. Peak boundaries and the beam current are not important due to the calculation of relative values. Results are presented in the following Tab. 5.1, including the data from MCNPX simulation, which are widely discussed in the next section.

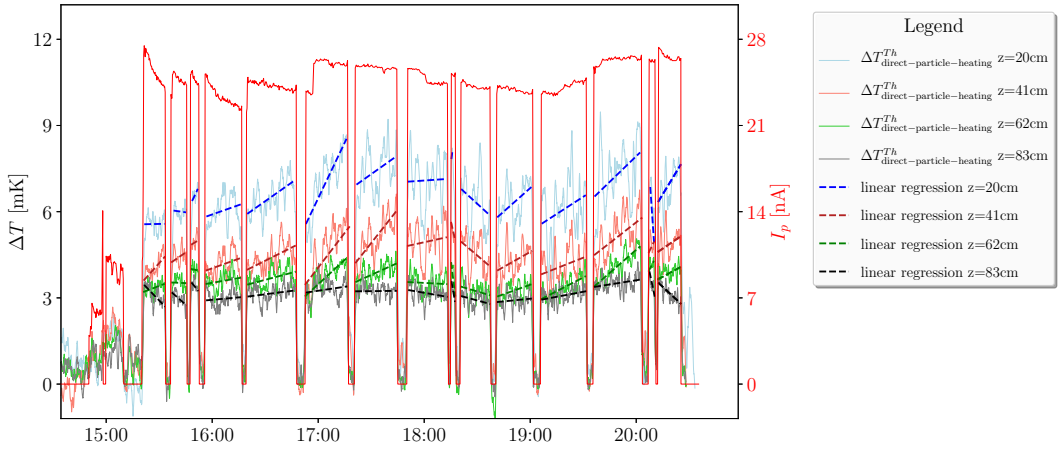

Figure 5.9: Direct particle reactions heating of the Th samples, monitored by temperature measured by highly accurate TC type E for the CARBON target irradiation.

Table 5.1: Relative comparison of the thorium sample direct heating

Method of the Th direct heating comparison	z=20cm	z=41cm	z=62cm	z=83cm
Relative ΔT measurement by TC type E	100%	70%	55%	48%
Relative heat deposition, MCNPX simulation	100%	78%	58%	46%

The comparison of ΔT relative values with rel. heat deposition values calculated by MCNPX can bring interesting ideas for future more detail study. If the beam changes are rapid enough (heat transfer delay is much longer) → temperature probes with a suitable sample might be very cheap detectors of the relative flux changes. In this case the thorium sample has been used, but in principle more common materials can be used.

5.2.2 Simulation of the CARBON target by MCNPX and ANSYS Fluent

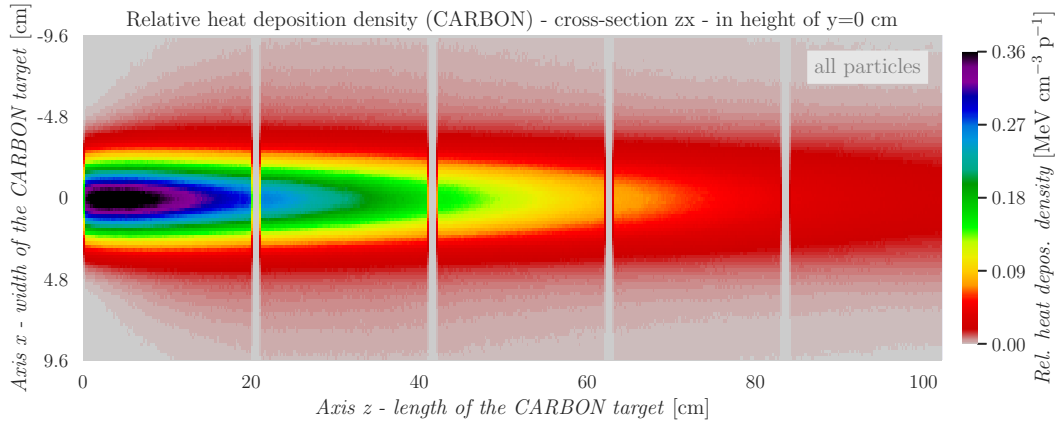

Figure 5.10: Relative heat deposition density of the CARBON target simulated by MCNPX - all heating particles are involved.

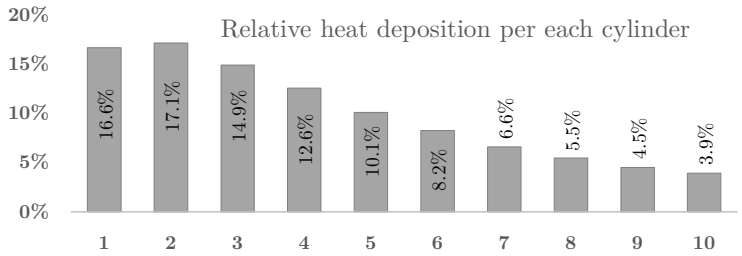

Figure 5.11: Relative heat generation per CARBON target cylinder.

ANSYS-FLUENT simulation setting and results

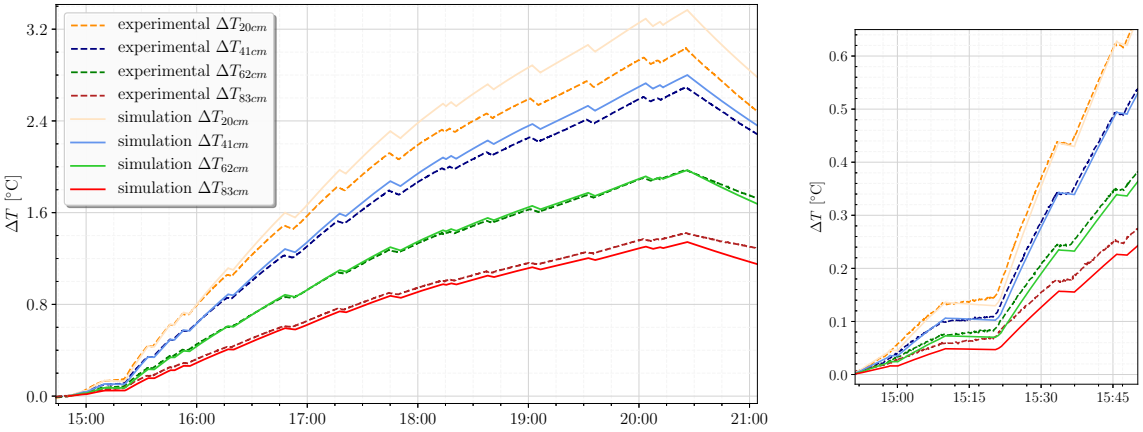

Figure 5.12: Comparison of the ΔT for simulation and measured data. On the left side is shown whole experiment time, right side figure shows zoomed part of the irradiation beginning. This simulation suffer of several inaccuracies, such as missing small block of thermal insulation between cylinders at measuring positions, slightly overestimated heat source, neglected experimental other samples and materials installed on the target surface, and primarily, neglected surrounding air temperatures changing during the experiment. For comparing purposes, the measured ΔT was offset to the beginning irradiation time, how ever it was not steady state, see zoomed part of Fig. 5.8. Results are widely described in the following discussion.

5.2.3 Results discussion - CARBON target

The CARBON target experiment consisted of several measurements. On the one side, there were offline monitoring of the neutron flux and its spectrum by an activation foil method (colleague research). On the other side, there were experiments based on very accurate temperature measurements. Unfortunately, the first-mentioned measurement affected the accuracy of the temperature measurement due to its requirement to have quick access to the target. For this reason, it was impossible to create ideal measuring conditions. However, this experiment was successful and brought many interesting results.

The proton beam instability was used for detailed monitoring of dynamical changes in the experimental setup, such as target cooling when the beam outage occurs, and primarily, the direct Th sample heating placed inside of the target. This part of the experiment studied a very cheap method of proton flux monitoring by accurate temperature measurement of two different materials. The ΔT of the CARBON target and thermally insulated Th samples were measured in a similar position at four different target lengths (different proton flux) and compared to the first measuring position. Based on the temperature measurement, which suffers from several simplifications, the relative proton flux was 70 %, 55 %, and 48 % for second, third, and fourth measuring positions. Based on the MCNPX simulation, the relative proton flux was 78 %, 58 %, and 46 % with respecting the previous order. It is a very interesting result of base research and should be more detailed studied in laboratory conditions. It can find usage in specific applications of proton or neutron flux occurrence monitoring. This method has many disadvantages, however, due to modern electronics, suitable utilisation can be found. The following research of this topic should be aimed at sensitivity analyses and experimental comparison of various materials in laboratory conditions with unified p/n flux source.

The heat generation monitoring of the cylindrical CARBON target irradiated by 660 MeV protons was carried out by accurate temperature measurement. These results were later compared with MCNPX simulation and ANSYS Fluent calculation. The utilisation of these tools is common - heat transfer simulations (ANSYS Fluent, OpenFOAM, Autodesk CFD, COMSOL Multiphysics, or others) are widely using in the industry, design and many other branches as well as particle transporting codes (MCNPX, Fluka, GEAT, or others), which are primarily used in medicine, science, industry and others. There are also applications, however, not so often, where these two totally different simulations are employed together, such as nuclear reactor design, spallation target experiments, or similar problems. In these cases, the heat is deposited by particle reactions in the simulated object and its transfer is monitored to ensure the limits of destruction (for experiments or testing) or to simulate transfer efficiency, structure stress, or others values. The CARBON target experiments (as well as the LEAD target) combine slightly complicated parts of these simulation possibilities - asymmetrical volume heat deposition which is various over irradiation time in combination with the simulation of natural convection heat transfer at lower temperature differences. Asymmetrical heat deposition was approximated by several equations generated from the written Python script, the variable behaviour over time was defined by Fluent User Defined Function (with using gamma-ray spectrometry method to estimate the total number of interacting protons, and accelerator ionisation chamber for relative proton beam monitoring over time). The most problematic part was the Fluent simulation. It took plenty of time, several consultations with ANSYS Fluent experts and a high number of sensitivity analyses to set the model and outer conditions accurately. Heat transfer simulation was also dependent on outside weather condition, which has been taken into account as well. Finally, the

comparison of experimentally measured data with purely simulated data was performed. There is one more problem in temperature measurement because one of our colleagues was carelessly installing some instruments on the front side of the experimental target, so the already stabled target temperature was interrupted. The whole target temperature increased for 0.06 °C, however, the first measuring section increased for 0.14 °C. It complicates the comparison due to the irradiation was not started in the target temperature steady-state. This problem is shown in zoomed Fig. 5.8 on the right side. For this reason, the ΔT offset is set to the time just before the irradiation starts.

The simulation reaches the maximal error during the irradiation of 11.1 % (in principle lower due to the discussed offset setting) for the highest temperature at the end of irradiation, see Fig. 5.12 (measured 3.0 °C, simulated 3.36 °C). For the second position, the maximal relative error is 3.9 %, for the 3^{rd} position it is 1.85 % and finally, for the 4^{th} 5.7 %. It is a very good result, moreover, if having in mind the complexity of this simulation placed in limited experimental conditions. The ANSYS Fluent simulation should be recalculated with a softer mesh, primarily in the upper target region (cells in the upper part are too large, the quality of the heat transfer simulation is not ensured). The model should be more accurate - thermal insulation and irradiation samples between sections are not simulated, which can increase the measured temperature in the lower temperature region. The approximated thermal power distribution is slightly overestimated. The internal thermal power distribution should be rather directly mapped from the MCNPX mesh tally results - it will be much more accurate and it includes asymmetrical power distribution. Unfortunately, this method (mapping) was unknown to the author at the beginning of the simulation process. The utilisation of approximated equations and UDF definition was very laborious, complicated, and finally, less accurate.

In summary, the used technique brought very interesting and pretty accurate results. It is possible to compare pure experimental data with the advanced simulation (a combination of several simulation + experimental methods).

Chapter 6

Conclusion

The extensive research performed in the frame of this PhD thesis goes through several topics. Experimental measurements were performed at JINR in Dubna and dealt with neutron and proton flux monitoring, gamma-ray spectrometry method, and accurate ΔT for the purpose of target heat generation monitoring. Research compares the experimental measurement with simulation. Data acquisition was performed by LabView. Experimental data were analysed by advanced Python scripts with various libraries usage - *pandas* and *numpy* for data manipulation and *matplotlib* and *seaborn* for visualisation, and other commonly used libraries. Irradiated samples and foils processed by gamma-ray spectrometry were measured by HPGe detectors in YaSNaPP laboratory at JINR.

Irradiated experiments were simulated by the particle transportation code MCNPX. The heat deposition was estimated per volume and as a volume mesh to estimate its distribution. The total number of protons interacting with the target was estimated by Cu and Al activation foil (gamma-ray spectrometry). Due to the proton beam being dynamic over time and the power distribution is proportional to the beam current, the dynamic power distribution was calculated based on the relative proton current monitored by gas-filled ionisation chambers. The transfer of the generated heat was simulated by ANSYS Fluent. The 3D specific heat distribution was approximated by several equations and interpreted by UDF to the Fluent. Time dependent experimental results were compared with the simulations. Although several simplifications are used, the experimental vs simulation uncertainty is about 11 % for the CARBON target and about 7.5 % for the LEAD target. If the simulation complexity is taken into consideration, the results are very sufficient. Moreover, the ANSYS Fluent calculation is going to be improved since academic licence is available. Based on the experience of 2D simulation, it is expected that the 3D Fluent simulation improvement by softening the mesh will be significant. When the MCNPX results will be mapped into the ANSYS and the source asymmetry will be taken into account, the uncertainty of simulation vs experiment is expected to be better than 5 % (with softer mesh of larger fluid volume).

Small proton beam current changes (such as 600 pA) for the LEAD target experiment were detected by the target ΔT measurement, as well as by neutron leakage heating probes. It means that the ΔI_p=600 pA causes a measurable change of the neutron flux in the radial distance 13.5 cm. Generally, the neutron leakage flux monitoring was carried out by ^{nat}U or ^{enr}U probes for the TA QUINTA and the LEAD target, where spallation neutron leakage occurs. For the TA QUINTA short irradiation, the direct internal heat increase comparison between the under third and second section was about 77 %. For long irradiation, the measurement is affected by several errors caused by the heat transfer from the TA QUINTA (difference thermal insulation) and the problem with TC connection - they were not connected to neighbour channels (CJ could reach slightly different temperature during the irradiation) due to the author mistake. Based on MCNPX simulation, the ratio of the heat deposition between these two positions is 84 %. It is very good correlation. The repetition of this experiment without the mentioned mistakes was planned but unfortunately, has not been performed yet. The lead neutron leakage monitoring by a similar technique reaches very good results.

The proton flux was measured by a similar method inside of the CARBON target. The relative proton flux was estimated by four tiny volume thorium probes. Probes were placed at four distances inside of the CARBON target. The uncertainty between the relative temperature comparison with MCNPX heat deposition simulation is about 11 % (if the MCNPX simulation reference), see p.22. The reached sensitivity was very high, the maximal measured ΔT was in this case merely 9 mK (with using a statistic function and data filtration). It must be stated that all of these experimental data comes from base experimental research and it should be studied in detail at laboratory conditions with unified sources. In principle, these results are a kind of parallel product of the main experimental heat generation research.

In summary, this kind of research was unique in the JINR ADS research group and brought important data about the opportunities and limits of these measurements. The author tested several methods and prepared a complete methodology of the measurement. There is included the thermocouples manufacturing, testing, and calibration. There are described troubles with data acquisition and its solutions. Due to larger data packages of measured and simulated data, there is a widely discussed Python scripting language utilisation. Most of the used scripts are enclosed, including a detail video manual enclosed on YouTube dissertation channel. Simulation by MCNPX, volume meshing, its visualisation, and primarily the method of 3D heat deposition distribution approximation by equations are widely discussed. The final solution is shared (uploaded to this thesis cloud). There is discussed the ANSYS Fluent simulation and its challenges. Due to dealing with natural convection in a large volume experimental hall, it is a very sensitive simulation. Detail manual of the model creation and setting is enclosed on YouTube as well. Many 3D models, simulations, and codes were made during this thesis processing - they are available on the Google Cloud Platform, based on BUT - Google cooperation. These files are accessible to all BUT students and academic staff. All links are listed in the last three pages of the appendix. These open access data hopefully help students to boost the learning process rapidity or help researchers to use the described programs and tools more easily due to enclosed tutorials.

Bibliography

[1] NASA. *Global Climate Change* [online]. 2020 [cit. 2020-02-15]. Available at: https://climate.nasa.gov/.

[2] Ritchie, H. and Roser, M. CO_2 and Greenhouse Gas Emissions. *Our World in Data*. 2020. Available at: https://ourworldindata.org/co2-and-other-greenhouse-gas-emissions.

[3] BP. *BP Statistical Review of World Energy 2019* [online]. Data Report. London: The British Petroleum Company plc, 2019. 64 p. [cit. 2020-02-25]. Available at: https://www.bp.com/content/dam/bp/business-sites/en/global/corporate/pdfs/energy-economics/statistical-review/bp-stats-review-2019-full-report.pdf.

[4] Smil, V. *Energy Transitions*. 1st ed. Praeger, 2010. ISBN 978–0–313–38178–2.

[5] Sovacool, B. K., Andersen, R. et al. Balancing safety with sustainability: assessing the risk of accidents for modern low-carbon energy systems. *Journal of Cleaner Production*. 2016, vol. 112, p. 3952 – 3965. Available at: https://doi.org/10.1016/j.jclepro.2015.07.059. ISSN 0959-6526.

[6] Smil, V. *Energy: A Beginner's Guide*. 2nd ed. Oneworld Publications, 2017. ISBN 1-786-07133-9.

[7] IAEA. *Energy, Electricity and Nuclear Power Estimates for the Period up to 2050*. IAEA, 2020. Available at: https://www.iaea.org/publications/14786/energy-electricity-and-nuclear-power-estimates-for-the-period-up-to-2050.

[8] Bouchet, S., Reitsma, F., Subki, M. and Kiuchi, H. Advances in small Modular Reactor Technology Developments. *IAEA Advanced Reactors Information System (ARIS)*. 2020. Available at: https://aris.iaea.org/Publications/SMR_Book_2020.pdf.

[9] Nifenecker, H., David, S., Loiseaux, J. and Meplan, O. Basics of accelerator driven subcritical reactors. *Nuclear Instruments and Methods in Physics Research Section A: Accelerators, Spectrometers, Detectors and Associated Equipment*. Elsevier. 2001, vol. 463, no. 3, p. 428–467.

[10] Bowman, C., Arthur, E., Lisowski, P., Lawrence, G., Jensen, R. et al. Nuclear energy generation and waste transmutation using an accelerator-driven intense thermal neutron source. *Nuclear Instruments and Methods in Physics Research Section A: Accelerators, Spectrometers, Detectors and Associated Equipment*. Elsevier. 1992, vol. 320, 1-2, p. 336–367.

[11] Rubbia, C. *Energy amplifier for nuclear energy production driven by a particle beam accelerator*. Google Patents, june 30 1998. US Patent 5,774,514.

[12] Asquith, N. *Fast and thermal Accelerator Driven Systems: Studies of secondary particle production and transport*. Sydney, 2015. 246 p. Dissertation. The University of Sydney, Faculty of Science.

[13] Závorka, L. *Transmutation of Actinides Using Spallation Reactions*. Prague, 2015. 168 p. Dissertation. Czech Technical University in Prague.

[14] Wilson, P. D. The nuclear fuel cycle from ore to wastes. 1996.

[15] Feiveson, H., Mian, Z., Ramana, M. and Hippel, F. von. Managing spent fuel from nuclear power reactors: Experience and lessons from around the world. *International Panel on Fissile Materials, available at: http://fissilematerials. org/library/rr10. pdf*. 2011.

[16] IAEA. Finland's Spent Fuel Repository a „Game Changer" for the Nuclear Industry. IAEA News Center. 2020, [cit. 2021-02-25]. Available at: https://www.iaea.org/newscenter/news/finlands-spent-fuel-repository-a-game-changer-for-the-nuclear-industry-director-general-grossi-says.

[17] Filges, D. and Goldenbaum, F. *Handbook of spallation research: theory, experiments and applications*. Wiley, 2009.

[18] Shen, B. S. P. and Merker, M. *Spallation nuclear reactions and their applications*. Springer Science & Business Media, 2012.

[19] Oxford University Press. *Oxford Dictionaries API* [online]. 2019 [cit. 2020-06-24]. Available at: https://www.lexico.com/.

[20] Katovský, K. *Studium sekundarních neutronů a jader vznikajících při reakcích protonů a neutronů v terči z uranu a plutonia*. Prague, 2008. 230 p. Dissertation. Czech Technical University in Prague.

[21] World Nuclear Association. *Accelerator-driven Nuclear Energy* [online]. 2019 [cit. 2020-02-08]. Available at: https://www.world-nuclear.org/information-library/current-and-future-generation/accelerator-driven-nuclear-energy.aspx.

[22] World Nuclear Association. *Status of Accelerator Driven Systems Research and Technology Development* [online]. 2015 [cit. 2020-03-11]. Available at: https://www-pub.iaea.org/MTCD/Publications/PDF/TE-1766_web.pdf.

[23] Yoshioka, R., Furukawa, K., Kinoshita, M., Degtyarev, A. M., Myasnikov, A. A. et al. 15 - Accelerator-driven systems. In: Dolan, T. J., ed. *Molten Salt Reactors and Thorium Energy*. Woodhead Publishing, 2017, p. 495–521. Available at: https://www.sciencedirect.com/science/article/pii/B9780081011263000154. ISBN 978-0-08-101126-3.

[24] ESS. *European Spallation Source-webside* [online]. 2020 [cit. 2020-10-22]. Available at: https://europeanspallationsource.se/.

[25] SKC·CEN. *MYRRHA* [online]. 2020 [cit. 2020-10-22]. Available at: https://www.myrrha.be/.

[26] IMP. *Introduction to ADANES Research in China* [online]. 2020 [cit. 2020-10-22]. Available at: http://english.imp.cas.cn/Work2017/CI2017/.

[27] Tichý, P. *Study of Accelerator-Driven Subcritical Setups Determined for Testing of Transmutation Possibilities*. Prague, 2020. 154 p. Dissertation. Czech Technical University in Prague.

[28] Bitter, R., Mohiuddin, T. and Nawrocki, M. *LabVIEW: Advanced programming techniques*. Crc Press, 2006.

[29] OMEGA. *TL-WELD* [online]. 2016 [cit. 2020-12-22]. Available at: https://br.omega.com/omegaFiles/heaters/pdf/TL_WELD.pdf.

[30] Chadwick, M., Herman, M., Obložinskỳ, P., Dunn, M. E., Danon, Y. et al. ENDF/B-VII. 1 nuclear data for science and technology: cross sections, covariances, fission product yields and decay data. *Nuclear data sheets*. Elsevier. 2011, vol. 112, no. 12, p. 2887–2996.

[31] Chadwick, M., Obložinskỳ, P., Herman, M., Greene, N., McKnight, R. et al. ENDF/B-VII. 0: next generation evaluated nuclear data library for nuclear science and technology. *Nuclear data sheets*. Elsevier. 2006, vol. 107, no. 12, p. 2931–3060.

[32] Junghans, A., De Jong, M., Clerc, H.-G., Ignatyuk, A., Kudyaev, G. et al. Projectile-fragment yields as a probe for the collective enhancement in the nuclear level density. *Nuclear Physics A*. Elsevier. 1998, vol. 629, 3-4, p. 635–655.

[33] Suchopar, M. *Study of neutron production and transport in systems based on spallation reactions*. Prague, 2016. 185 p. Dissertation. Czech Technical University in Prague.

Abstract:

Sub-critical Accelerator-Driven Systems (ADS) technology is able to deal with spent nuclear fuel (SNF) of present nuclear reactors, by using transmutation technique of long-lived radioactive isotopes. As well, the ADS technology is solving the potential problem with the lack of ^{235}U by possible utilisation of ^{238}U or abundant ^{232}Th. This doctoral thesis deals with research on the topic of spallation reaction and heat generation of various experimental targets in the frame of base ADS research. All experiments, in total 13, have been performed at Joint Institute for Nuclear Research (JINR) in Dubna, Russian Federation, during years 2015-2019. Various targets were irradiated as 512 kg of natural uranium target QUINTA, elongated cylindrical lead target and carbon target, or lead bricks target by 660 MeV protons at the irradiation facility Phasotron at JINR. A special experiment was performed with irradiation of two small $^{\mathrm{nat}}$U cylinders the QUINTA consist of. The author mostly investigates the heat generation by proton reactions (inelastic scattering, and ionisation looses) which are part of spallation reaction including Coulomb scattering (or Rutherford scattering, which represents elastic scattering of charged particles); neutron reaction (mostly contributed by fission); pion$^+$ reaction; and finally gamma heating, the heat generated by photon capturing. The temperature was experimentally measured by highly accurate and specially calibrated thermocouples. The temperature was measured as on the surface, so inside of the target. Additional research was aimed at neutron leakage monitoring by ΔT measurement of tiny volume probes by accurate thermocouples. The first probe contains a small amount of fissile material and the second one of non-fissile material with similar material characteristics. Leaking neutrons (neutron flux outside of the target) were detected due to direct heating of fission reactions. This work deals with accurate temperature measurement by thermocouples. It uses the LabView software for data acquisition, the National Instrument hardware for measuring, and Python 3.7. for data manipulation, analysing and visualisation (with employing several libraries). The particle transportation is simulated by MCNPX 2.7.0. and finally, the heat transfer and surface temperature estimation are simulated by ANSYS Fluent (or ANSYS Transient Thermal for simpler problems).

JOSEF SVOBODA

PhD student at Brno University of Technology
Researching internship at JINR in Dubna, Russia

CONTACT

josef.svoboda@vut.cz
+420 541 146 247
Technická 12, Brno, Czechia
BUT, Brno

Josef Svoboda
Josef Svoboda
List of publications

SKILLS

Programming

Python
LaTeX

Operating Systems

Linux
MacOS
Windows

Software & Tools

Visualisation
(e.g. matplotlib, gnuplot, seaborn ...)
Data handling/analysis
(e.g. numpy, scipy, pandas, ...)
ANSYS CFD
CAD - Inventor, SketchUp
Genie 2000
LabView
MCNPX
MS Office
Photoshop

Another skills

Gamma-spectrometry method
HPGe detector utilisation

Languages

Czech (native)
English (C1)
Russian (B2)
Spanish (A1)

CERTIFICATES

Radiation protection workshop
Indian Monte Carlo workshop

RESEARCH TOPICS

2013 → 2015:
○ RTG generators, α decay for space, β^- remote lighthouses
○ nuclear pacemakers
○ phase change materials - NPP safety, ice condenser containment
○ Th utilisation in conventional PWR reactor + MCNP criticality simulation + experimental reactor irradiation

2015 → 2020:
•**proton beam monitoring by gamma-spectrometry**
•neutron leakage monitoring by invented temperature probes
•**spallation target (ST) heat generation monitoring**
•rel. neutron flux determination of ST by ΔT probes
•**ST heat generation** •data acquisition (LabView)
•**ST simulation in MCNPX** •CAD modelling
•**Python data processing** •ANSYS CFD calculation,

EDUCATION

09/2015 - 06/2021 (expected)
BUT, Brno, Czech Republic
Doctor of Philosophy
Experimental research of various spallation targets heat generation.

01/2014 - 06/2015
BUT, Brno, Czech Republic
Master of Power Engineering
Diploma thesis: Possibility of thorium utilisation in current NPPs.

09/2013 - 01/2014
VGTU, Vilnius, Lithuania
Master of Power Engineering
The Erasmus Programme - exchange program for studying part of MSE abroad.

09/2010 - 06/2013
BUT, Brno, Czech Republic
Bachelor of Power Engineering
Bachelor thesis: Alternative Sources of Nuclear Energy; focused on nuclear power sources
in space and remote locations, chiefly Radioisotope Thermoelectric Generator (RTG)
→ Bachelor thesis was awarded by the Dean for extraordinary contribution.

PHD RESEARCH WORK BALANCE